Additive-Driven Phase-Selective Chemistry in Block Copolymer Thin Films: The Convergence of Top–Down and Bottom–Up Approaches**

By *Phong Du*, *Mingqi Li*, *Katsuji Douki*, *Xuefa Li*, *Carlos B. W. Garcia*, *Anurag Jain*, *Detlef-M. Smilgies*, *Lewis J. Fetters*, *Sol M. Gruner*, *Ulrich Wiesner*,* and *Christopher K. Ober**

The routine formation of nanometer-sized structures remains a challenge that limits advances in many fields of nanotechnology. Increasingly "bottom–up" self-assembly approaches for the nanometer-scale patterning of surfaces are competing with traditional "top–down" lithographic processes such as scanned-probe lithography or high-resolution electron-beam (e-beam) lithography. Block copolymer thin films (< 100 nm) are among the more promising materials being examined as they offer ease of processing combined with phase separation induced structure formation on the nanometer scale.

Recent work in block copolymer thin film pattern formation has included the use of poly(styrene-*block*-isoprene) to form periodic structures combined with ozonolysis to remove the isoprene phase, thereby creating arrays of holes in the polymer thin film.[1] In another case, poly(styrene-*block*-methyl methacrylate) has been processed in electric fields to align a cylinder phase perpendicular to the film surface, and subsequently exposed to UV light to both mildly crosslink the styrene phase and degrade the methyl methacrylate domains.[2] Similar strategies have been employed to process other block copolymer systems that contain a variety of chemical structures and architectures.[3] Examples of desirable target applications of such porous thin films include photonic bandgap materials, structures to serve as molecular sieves, or templates for magnetic structures.[4]

A typical means for improving the processing of bulk polymers is through the use of small-molecule additives.[5] While such additives in bulk polymer structures are ubiquitous, their application in block copolymer thin film processing has not been substantially explored to date. Given the enormous numbers of property variations possible this is surprising. Here we will show several strategies for the use of additive-driven chemistries that take place in only one type of the nanosized domains of block copolymer thin films. We then use such an approach to examine the convergence of "top–down" with "bottom–up" fabrication through light-driven processes.

In Figure 1, the structures of the three polymer systems and their respective phase selective additives are introduced. They are: (system 1) poly(α-methyl styrene-*b*-4-hydroxystyrene) (P(αMS-*b*-HOST)) and tetramethoxymethyl glycuril (TMMU) with photoacid generator; (system 2) poly(α-methyl styrene-*b*-isoprene) (P(αMS-*b*-I)) and 2,4,6-trimethylbenzoyl-diphenylphosphine oxide (TPO); and (system 3) poly(isoprene-*b*-ethylene oxide), (P(I-*b*-EO)) and 3-glycidoxypropyl-trimethoxysilane/aluminum *sec*-butoxide (GLYMO)/ $Al(O^sBu)_3$. While the first two systems are all-organic, in the case of P(I-*b*-EO) inorganic additives were used. All polymers were produced using living anionic polymerization, because of its excellent control of architecture and molecular weight (Fig. 1). Films of various controlled thicknesses down to monolayer (see below) were obtained by spin-coating from dilute solution onto silicon wafers.

Selection of the appropriate chemistry makes it possible to tailor the role of each block. In the P(αMS-*b*-HOST) system 1, the 4-hydroxy styrene (HOST) is rendered insoluble by photoacid-induced crosslinking with TMMU[6] and the αMS block is removed through UV/vacuum treatment. The P(αMS-*b*-HOST) polymer was combined with both TMMU (4 wt.-%) and a photoacid generator, triphenylsulfonium trifluoromethyl sulfonate (1.6 wt.-%) and deposited from solution on a silicon wafer. Exposure to low levels of 248 nm UV radiation (~ 10 mJ cm^{-2}) leads to efficient crosslinking of the HOST phase. UV light triggers the generation of acid by the photoacid generator that in turn catalyzes the reaction of the TMMU with the hydroxy group to crosslink the HOST block. Regardless of the local distribution of the reactants, this chemistry only takes place in the HOST phase. In the case of the P(αMS-*b*-I) block copolymer (system 2) the isoprene domain is radically crosslinked by the TPO[7] photoradical generator while the αMS block is removed during subsequent UV photolysis. Crosslinking under mild UV exposure (~ 100 mJ cm^{-2}) renders the continuous isoprene phase stable

[*] Prof. U. Wiesner, Prof. C. K. Ober, P. Du, M. Li, K. Douki,[+] X. Li, C. B. W. Garcia, A. Jain
Department of Materials Science and Engineering, Cornell University
Bard Hall, Ithaca, NY 14853 (USA)
E-mail: ubw1@cornell.edu; cober@ccmr.cornell.edu

Dr. D.-M. Smilgies
Cornell High Energy Synchrotron Source (CHESS), Cornell University
Ithaca, NY 14853 (USA)

Prof. L. J. Fetters
Department of Chemical and Biomolecular Engineering, Cornell University
Olin Hall, Ithaca, NY 14853 (USA)

Prof. S. M. Gruner
Department of Physics, Cornell University
Clark Hall, Ithaca, NY 14853 (USA)

[+] Present address: JSR Micro, Inc., Sunnyvale, CA 94089, USA.

[**] We gratefully thank Dr. Kathryn W. Guarini and Dr. Charles T. Black for helpful discussions, Dr. Jochen S. Gutmann for stimulating discussions about GISAXS data collection and interpretation and Dr. Ernest Fontes for his help with the CHESS experimental setup and support. The financial support by the Cornell Center for Materials Research (CCMR), a Materials Research Science and Engineering Center of the National Science Foundation (DMR-0079992), the NSF-funded Cornell NIRT (ECS-0103297-NIRT), the National Science Foundation (Grants DMR-0072009 and DMR-0072009), the IBM Faculty Partnership Program, and JSR Corporation is acknowledged. CHESS is a national user facility supported by NSF/NIH-NIGMH grant DMR-9713424. This work was supported in part by the Nanobiotechnology Center (NBTC), an STC Program of the National Science Foundation under Agreement No. ECS-9876771.

DOI: 10.1002/adma.200306189
© 2004 WILEY-VCH Verlag GmbH & Co. KGaA, Weinheim

ADVANCED MATERIALS

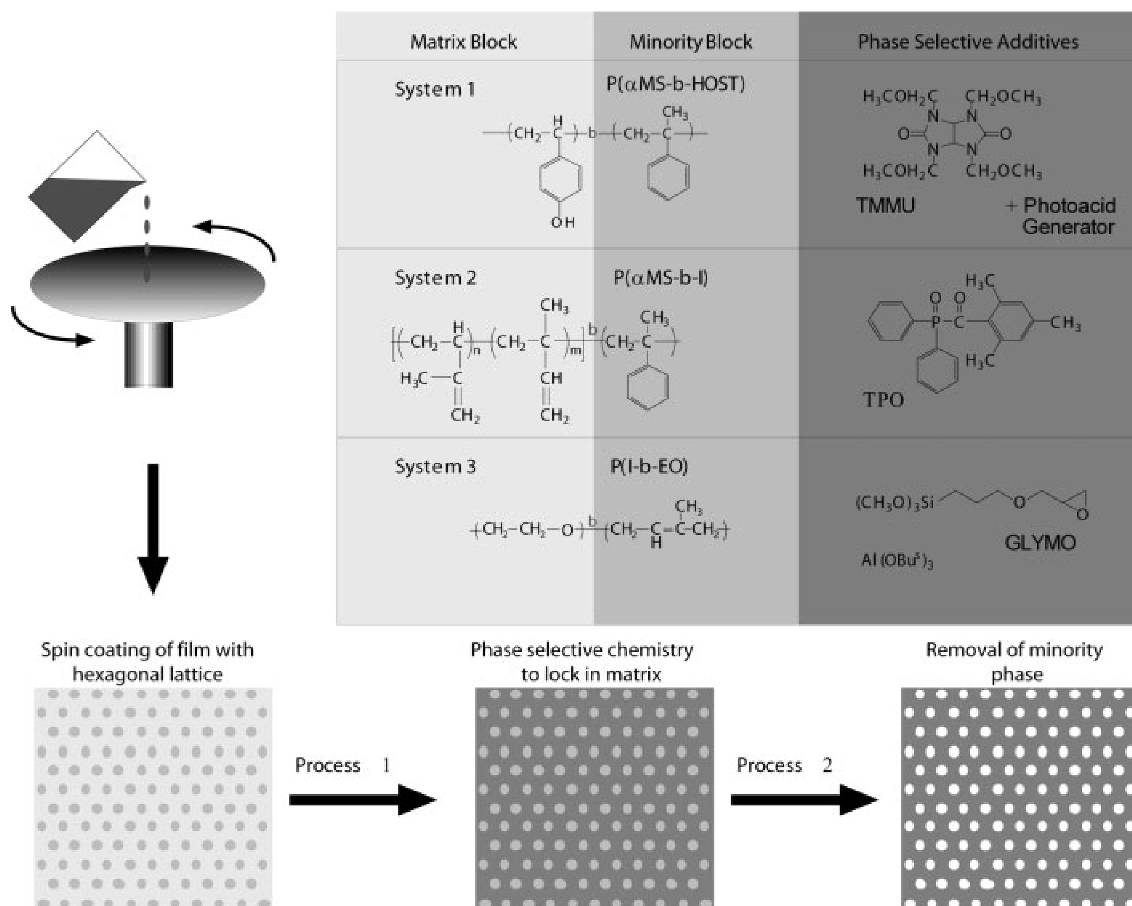

Figure 1. The three polymer systems examined in this study: (system 1) poly(α-methyl styrene-*b*-4-hydroxystyrene), P(αMS-*b*-HOST), contains a 4-hydroxystyrene matrix block which is photocrosslinked with TMMU and photoacid generator; (system 2) poly(α-methyl styrene-*b*-isoprene), P(αMS-*b*-I), is photocrosslinked with TPO. Both systems 1 and 2 have removable α-methyl styrene blocks; in (system 3) poly(isoprene-*b*-ethylene oxide), P(I-*b*-EO), the PEO block serves as the site for reaction with GLYMO/Al(O^{s}Bu)$_3$ and is eventually removed with all other organic components. As shown in the schematic, all systems share processing via spin-coating, which ultimately leads to pores penetrating from the top to the bottom of the films, see Figure 2. Subsequent processing locks in the matrix and removal of the minority phase leads to porous thin films.

enough that when further UV exposure (>300 mJ cm^{-2}) with vacuum is used to degrade the αMS phase, matrix phase collapse does not occur. Via the appropriate selection of additive chemistry, the isoprene block can serve as either the retained block as in system 2 or a removable component as in system 3. In the latter, the ethylene oxide microphase of the P(I-*b*-EO) block copolymer is swollen by the inorganic precursors serving as host for the sol–gel-derived aluminosilicate products.[8] Subsequent high-temperature oxidation removes all organic components leaving a pure oxide film. Going from all-organic systems 1 and 2 to a system with inorganic additives (system 3) opens additional opportunities such as high-temperature processing or extended etching capabilities unavailable for all-organic thin films.

Thin film morphologies of these three systems as observed by atomic force microscopy after processing is shown in Figures 2A–C (height mode images). In all cases a hexagonal arrangement of pores can be observed. Please note that although the chemistries in each case are quite different, we were able to achieve similar microstructures without special surface treatment. Although not shown, the arrangement and size of these pores corresponds very well to those of the as-made, unprocessed block copolymer thin film microstructures. Figure 2D shows a cross-section of the same film depicted in Figure 2C, system 3, but before high-temperature oxidation. The cross section image shows the sample upside down, i.e., the silicon substrate is above the film and the surface revealed in Figure 2C is pointing downwards (the hexagonal pore arrangement is thus not visible). Figure 2D clearly demonstrates that monolayer control can be achieved in these thin films.

In order to test the thin film structures on macroscopic length scales and to demonstrate that the atomic force microscopy (AFM) images of Figure 2 are representative, we employed grazing-incidence small-angle X-ray scattering (GISAXS)[9] on all samples. Measurements were performed at the Cornell High Energy Synchrotron Source (CHESS) D-line featuring a multilayer monochromator and an area detector. Here we will only discuss the results of system 3. In

 © 2004 WILEY-VCH Verlag GmbH & Co. KGaA, Weinheim

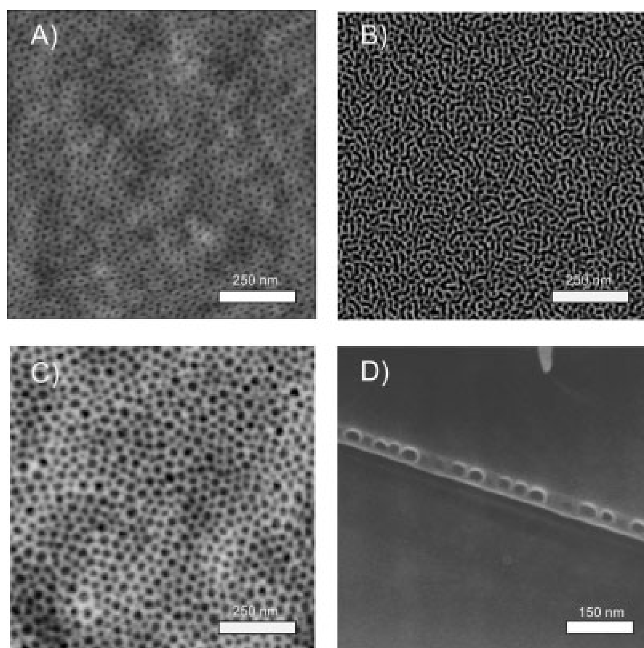

Figure 2. AFM height images of porous thin films produced from A) (system 1) P(αMS-*b*-HOST) + TMMU with photoacid generator, B) (system 2) P(αMS-*b*-I) + TPO, and C) (system 3) P(I-*b*-EO) + GLYMO/Al $(O^sBu)_3$. In each system porous structures are produced using phase-specific chemistry. The pore dimensions are consistent with the size of the starting film microstructures. D) A SEM image of system 3 shows the arrangement of the microstructure prior to calcination demonstrating monolayer control.

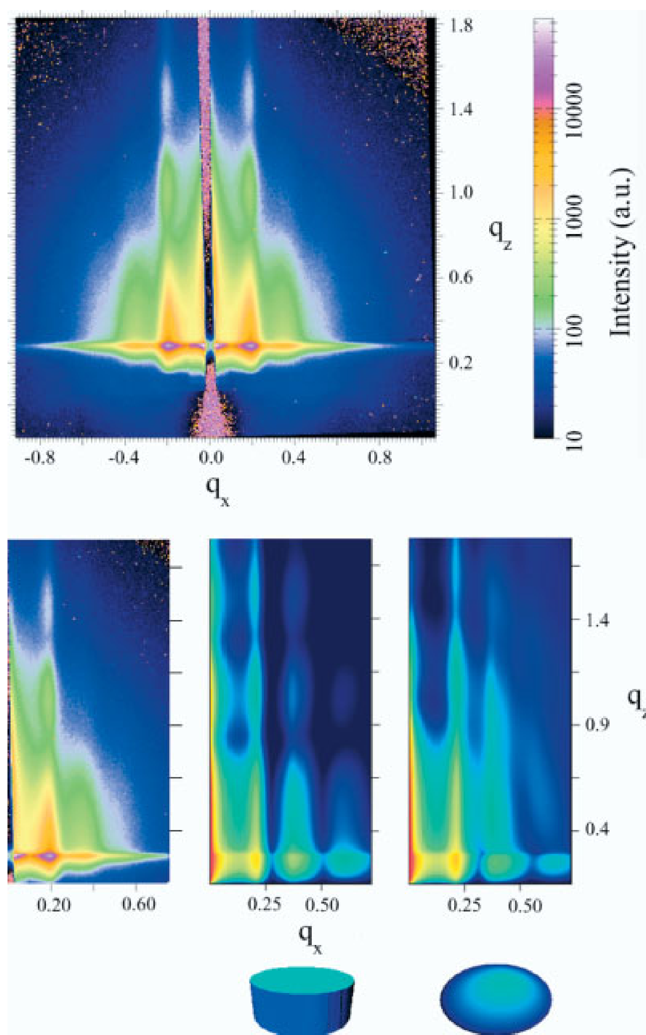

Figure 3. A) Experimental GISAXS scattering pattern from a monolayer-type calcined film as shown in Figure 2. B) Comparison of experimental (left) and simulated scattering patterns. q-values are in reciprocal nanometers, with q_x parallel, and q_z perpendicular to the plane of the polymer film. Two scattering object geometries were employed in the simulation, namely cylinders and ellipsoids as indicated below the respective images. Input parameters for the simulations were: pore–pore spacing (34.6 nm), film thickness (14 nm), and aspect ratio (height/radius = 1). These values were consistent with those obtained from the other characterization techniques (AFM and SEM). A Gaussian probability distribution was applied to input parameters to better simulate experimental conditions. X-rays of wavelength $\lambda = 0.155$ nm incident at 0.2075° to the film surface were used. The scattering objects (representing the pores) were distributed on a regular hexagonal lattice. Application of cumulative disorder, as described in the IsGISAXS simulation package, resulted in a loss of long-range order, consistent with AFM data (see Fig. 2). The IsGISAXS simulation package is available from ESRF [10].

Figure 3, a GISAXS pattern is shown for the calcined state (after removal of all volatile components). In these experiments, lateral correlations within the film plane and structural information along the film normal are documented through scattering intensity in the q_x and q_z directions of the two-dimensional scattering patterns, respectively. As expected the scattering intensity is significant due to strong electron-density contrast between the pores and the inorganic phase. Scattering intensity along q_x is observed up to higher orders. In addition, the calcined film shows a distinct scattering intensity modulation along the q_z direction. Since the film is a monolayer, as evidenced by the scanning electron microscopy (SEM) image in Figure 2D, this modulation can only be attributed to the form factor of the scattering objects, i.e., the pore geometry.

The 2D GISAXS results were simulated employing the software package IsGISAXS.[10] Simulation results for the calcined film for two different pore geometries, i.e., cylinder and ellipsoid, are shown at the bottom of Figure 3. Overall the observed intensity distribution in the 2D plane is very well reproduced. For the ellipsoidal pore structure simulation, curvature towards the main beam reflection occurs, in particular for the higher-order peaks. This is not observed in the experimental data. Since the effect is most pronounced for high q-values, additional experiments were performed, in which the low q-range was blocked and data only for the high q-range was acquired. No curvature could be observed in these experiments either. Rather, the results are better represented through the cylindrical pore model for which the intensity distribution along q_z is a straight line, consistent with the data. Pore structure dimensions obtained from all simulations are in good agreement with experimental results from AFM and SEM.

 © 2004 WILEY-VCH Verlag GmbH & Co. KGaA, Weinheim

The preceding results show that additive-driven phase-selective chemistry can be used to create nanostructured thin films. These films are interesting in their own right, but here we would like to go one step further towards an application of this concept that combines this "bottom–up" approach with a lithographic "top–down" approach. This combination enables hierarchical structure formation in thin films from the macroscale down to the nanoscale. In order to explore the prospects for the use of phase-selective chemistry in lithography, the P(αMS-*b*-HOST) block copolymer was investigated as a photoresist. Random copolymers based on PHOST are the workhorse of the semiconductor industry and are the basis for many chemically amplified, high-resolution resists. Figures 4A,B show both the chemistry of the lithographic process and an AFM of the surface of the polymer mixture before (A) and after (B) exposure to UV radiation. A comparison of the AFM images in Figure 4 shows that the microstructure of the block copolymer thin film is not altered by the lithographic process. The same low levels of 248 nm UV radiation that lead to crosslinking of the PHOST phase also permit patterning of this polymer as a very efficient negative resist system as shown in Figure 4C. In the unexposed regions, the PHOST block remains soluble in aqueous base (0.26 N tetramethylammonium hydroxide (TMAH)) whereas the exposed region is crosslinked and insoluble. A range of exposure doses and test patterns were examined and Figure 4C demonstrates that this polymer system can produce patterns on the order of 400 nm making this material a high-resolution resist in its own right. A subsequent, longer exposure to UV radiation in a modest vacuum leads to removal of the PαMS phase with formation of vacant pores that lie within the patterned regions as in Figure 2A.

This report demonstrates that the use of additive-driven thin-film phase-selective chemistry permits direct coupling of a well-established "top–down" lithographic approach to "bottom–up" self-assembly of block copolymers. These materials are presently being explored as supported porous thin films to separate proteins of selected molecular weight ranges. One can also envisage such materials for template formation for a variety of uses.

Experimental

Polymer Synthesis: (PαMS-*b*-HOST): Block copolymers of poly(α-methylstyrene-*b*-4-*tert*-butoxystyrene), PαMS-*b*-P*t*BuOS, were synthesized by sequential anionic polymerization in tetrahydrofuran (THF) at –78 °C with *sec*-butyl lithium as the initiator. The α-methylstyrene monomer was polymerized first for 12 h and an aliquot of poly(α-methyl styryl lithium) was isolated for analysis after termination with degassed methanol. The 4-*tert*-butoxystyrene (*t*BuOS) monomer was then introduced into the reactor and the reaction was terminated with degassed methanol after 12 h. The PαMS-*b*-*t*BuOS was converted to poly(α-methylstyrene-*b*-4-hydroxystyrene), PαMS-*b*-HOST, by a hydrolysis reaction. The block copolymer was first dissolved in dioxane, and a ten-fold amount of hydrochloric acid was added. The reaction continued at 80 °C under an atmosphere of nitrogen overnight and then precipitated into water. After neutralization with a 5 wt.-% NaOH solution to pH 6–7, the resulting polymer was filtered and dried under vacuum at room temperature. The resulting polymer underwent a dissolution-precipitate cycle from a THF solution to methanol/water (v/v = 1:1) mixture twice and finally freeze-dried from dioxane. Characterization by gel permeation chromatography (GPC) and ^{1}H NMR revealed a composition of 28.5 % PαMS by weight and molecular weight of 45 400 g mol^{-1} (polydispersity index (PDI) ~ 1.1).

P(αMS-*b*-I): The asymmetric diblock copolymer poly(α-methyl styrene-*b*-isoprene) was kindly provided by Lewis Fetters, then at Exxon. Characterization by GPC and ^{1}H NMR revealed a composition of 25 % PαMS by weight and molecular weight of 64 000 g mol^{-1} (PDI ~ 1.1).

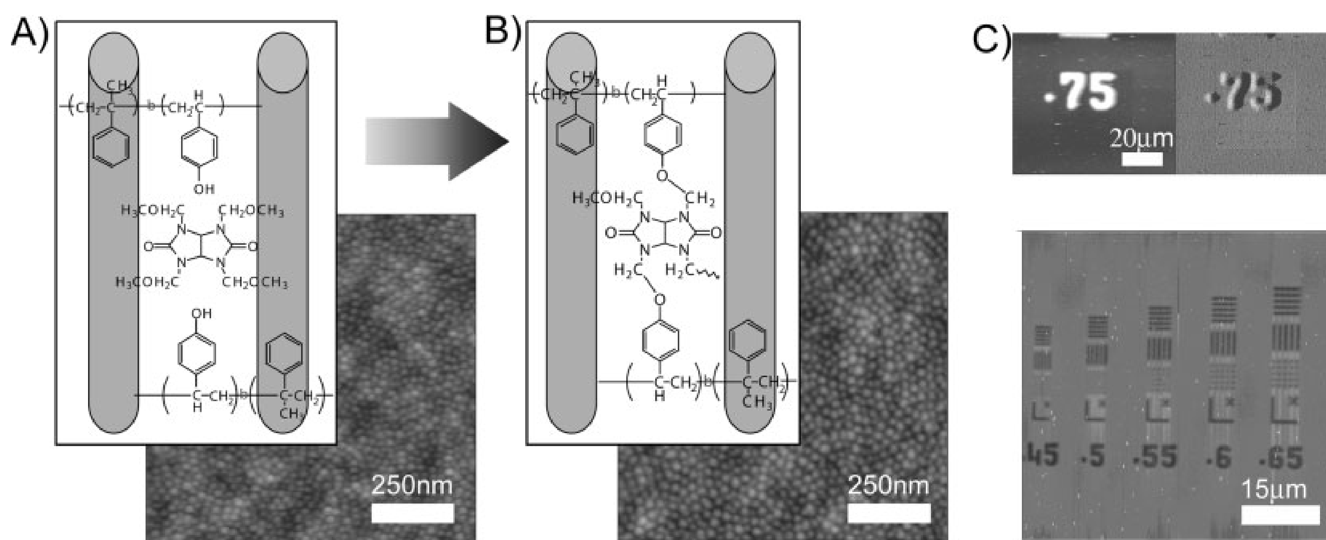

Figure 4. The process for patterning the P(αMS-*b*-HOST) block copolymer involves photochemical crosslinking with TMMU in combination with photoacid generator. Prior to crosslinking (A) the block microstructure shows hexagonal order as revealed by phase contrast AFM. After photocrosslinking (B) further AFM studies show the microstructure and its orientation are retained. By development in aqueous base, the unexposed regions can be easily dissolved to form patterned sub-micrometer images. The upper portion of (C) shows a test pattern in which pores have been formed during subsequent processing. A more detailed image of a nanoporous film is shown in Figure 2A. The lower portion of C shows a lithographic image with features as small as 450 nm.

 © 2004 WILEY-VCH Verlag GmbH & Co. KGaA, Weinheim

P(I-*b*-EO): The block copolymer P(I-*b*-EO) was synthesized using anionic polymerization as described in [11]. Characterization by GPC and ^{1}H NMR revealed a composition of 32 % poly(ethylene oxide) (PEO) by weight and molecular weight of 38 700 g mol^{-1} (PDI < 1.1).

Nanofabrication: (PαMS-*b*-HOST): A sample of the PαMS-*b*-HOST block copolymer was dissolved with a small amount of tetramethoxymethyl glycouril (4 wt.-%) as a crosslinker (CL) and triphenylsulfonium trifluorosulfonate (1.6 wt.-%) as a photoacid generator (PAG) in propylene glycol methyl ether acetate (PGMEA). Spin-coating of the mixture onto a silicon substrate produced vertically aligned cylinder nanodomains over the entire substrate. By irradiation through conventional photomasks and subsequent mixed solvent development, a high resolution photopattern was generated. Subsequent strong UV irradiation on the developed pattern activated the depolymerization process of the PαMS building block, forming nanosized holes in spatially controlled micrometer-sized patterns. Photoimaging experiments were performed using a Nikon 248 nm stepper (numerical aperture (NA) = 0.42 and σ = 0.5) equipped with a KrF excimer laser (Cymer CX-2LS) in the Cornell Nanofabrication Facility for the first exposure. Subsequent exposure with a JBA 1000 DUV Resist Cure Ramp (450 mJ cm^{-2} at 250 nm) followed by heating (115 °C for 60 s) was used to crosslink the PHOST matrix. A mixed solvent (cyclohexanone/isopropanol = 1:2 in volume) was used as a developer to form the negative-tone photoresist patterns. The thickness of the polymer films was examined with a P-10 profilometer. A second irradiation step (70 J cm^{-2} at 365 nm) was carried out to remove the PαMS block at 80 °C under high vacuum (~ 9 × 10^{-5} torr).

(PαMS-*b*-I): Poly(α-methyl styrene-*b*-isoprene) was mixed with 3 wt.-% photoinitiator 2,4,6-trimethylbenzoyldiphenylphosphine oxide, provided by BASF (Product name: Lucirin TPO) to crosslink the poly(isoprene) matrix before the degradation of the cylindrical α-methyl styrene phase. This phosphine oxide is ideal because it has two main advantages over other types of photoinitiators: high light absorbance and fast photobleaching. A UV source (model SCU 110B from UVEX corporation) was used to crosslink the isoprene block using a peak intensity of λ = 365 nm during exposure of 3 min. A film of the polymer was spin-coated from a solution of block copolymer and TPO in PGMEA. Subsequent strong UV irradiation on the polymer film activated the depolymerization process of the PαMS building block, forming nanometer-sized holes in spatially controlled micrometer-sized patterns.

P(I-*b*-EO): Samples were prepared by spin-coating (CEE Model 100CB, velocity: 2000 rpm, duration: 53 s) onto silicon wafers from a 0.5 wt.-% PI-*b*-PEO polymer solution of equal weight THF/chloroform with a specific amount of added inorganic species (GLYMO/Al(O^{s}Bu)$_3$). Crosslinking of the film was achieved in a vacuum oven at 130 °C for 1 h. Subsequent calcination was carried out in a furnace at 500 °C (temperature ramp: 5 °C min^{-1}) to remove the organic components.

Characterization: AFM data for Figures 2A,B were captured using a Veeco Dimension 3100 Scanning Probe Microscope operated in tapping mode with Olympus TappingMode Etched Silicon probes (resonant frequency = 300 kHz, force constant = 42 N m^{-1}, tip radius of curvature = 10 nm; all values nominal) under ambient conditions. AFM data for Figure 2C was captured using a Veeco Nanoscope III MultiMode Scanning Probe Microscope operated in tapping mode with TappingMode Etched Silicon probes (resonant frequency = 325 kHz, force constant = 37 N m^{-1}, tip radius of curvature = 10 nm; all values nominal) under ambient conditions. SEM data for Figure 2D was captured using a Hitachi S4500 Field Emission Scanning Electron Microscope with an acceleration voltage of 5 kV and working distance of 10 mm. GISAXS data of system 3 samples were collected with a 2D area detector (X-ray energy: 8 keV, sample-to-detector distance: 106 cm, angle: ~ 0.2°, exposure time: 1–10 s).

Received: September 17, 2003
Final version: February 2, 2004
Published online: June 3, 2004

[1] M. Park, C. Harrison, P. M. Chaikin, R. A. Register, D. H. Adamson, *Science* **1997**, *276*, 1401.
[2] T. Thurn-Albrecht, R. Steiner, J. DeRouchey, C. M. Stafford, E. Huang, M. Bal, M. Tuominen, C. Hawker, T. P. Russell, *Adv. Mater.* **2000**, *12*, 787.
[3] a) M. A. Hartney, A. E. Novembre, F. S. Bates, *J. Vac. Sci. Technol. B* **1985**, *5*, 1346. b) D. Zhao, P. D. Yang, N. Melosh, Y. L. Feng, B. F. Chmelka, F. Stucky, *Adv Mater*. **1998**, *10*, 1380. c) V. Z.-H. Chan, J. Hoffman, V. Y. Lee, H. Iatrou, A. Avgeropoulos, N. Hadjichristidis, R. D. Miller, E. L. Thomas, *Science* **1999**, *286*, 1716. d) K. Yu, B. Smarsly, C. J. Brinker, *Adv. Funct. Mater.* **2003**, *13*, 47.
[4] a) T. Thurn-Albrecht, J. Schotter G. A. Kastle, N. Emley, T. Shibauchi, L. Krusin-Elbaum, K. Guarini, C. T. Black, M. Tuominen, T. P. Russell, *Science* **2000**, *290*, 2126. b) A. Urbas, R. Sharp, Y. Fink, E. L. Thomas, M. Xenidou, L. J. Fetters, *Adv. Mater*. **2000**, *12*, 812. c) K. Asakawa, T. Hiraoka, H. Hieda, M. Sakurai, Y. Kamata, K. Naito, *J. Photopolym. Sci. Technol*. **2002**, *15*, 465.
[5] K. Yurekli, R. Krishnamoorti, M. F. Tse, K. O. McElrath, A. H. Tsou, H.-C. Wang, *J. Polym. Sci. B* **2001**, *39*, 256.
[6] J. D. Gelorme, N. C. Labianca, W. E. Conley, S. J. Holmes, *IBM J. Res. Dev.* **1997**, *41*, 81.
[7] C. Decker, K. Zahouily, D. Decker, T. Nguyen, T. Viet, *Polymer* **2001**, *42*, 7551.
[8] a) P. F. W. Simon, R. Ulrich, H. W. Spiess, U. Wiesner, *Chem. Mater*. **2001**, *13*, 3464. b) P. Du, J. S. Gutman, P. F. W. Simon, C. B. W. Garcia, K. Guarini, C. T. Black, U. Wiesner, *Polym Prepr. (Am. Chem. Soc., Div. Polym. Chem.)* **2002**, *43*, 438.
[9] D.-M. Smilgies, P. Busch, C. M. Papadakis, D. Posselt, *Synchrotron Radiation News* **2002**, *15*, 35.
[10] R. Lazzari, *J. Appl. Cryst.* **2002**, *35*, 406. A copy of the software can be downloaded from: http://www.esrf.fr/computing/scientific/joint_projects/IsGISAXS/
[11] J. Allgaier, A. Poppe, L. Willner, D. Richter, *Macromolecules* **1997**, *30*, 1582.

Nanoseparated Polymeric Networks with Multiple Antimicrobial Properties**

By *Chau Hon Ho*, *Jan Tobis*, *Christina Sprich*, *Ralf Thomann*, and *Joerg C. Tiller**

The increasing demand for hygienic living conditions leads to a great need of antimicrobial materials that do not allow microbes to attach, survive, or at least proliferate on material surfaces. Such materials lower the risk of transmitting diseases, poisoning the environment, or biofouling materials. Three main approaches have been applied to render materials

[*] Dr. J. C. Tiller, C. H. Ho, J. Tobis, C. Sprich, Dr. R. Thomann
Freiburg Materials Research Center
Stefan-Meier-Str. 21, D-79104 Freiburg (Germany)
E-mail: joerg.tiller@fmf.uni-freiburg.de

[**] The authors are grateful to the Deutsche Forschungsgemeinschaft for financing the young scientist research group of JCT (Emmy-Noether-Program). The work was further financially supported by the DFG (SFB428/A2) and the Fonds der Chemischen Industrie. The authors thank Dr. Yi Thomann for help with the AFM images, Sigrid Hirth-Walter for performing the AAS measurements, and Dr. Klaus Pelz for providing the *S. aureus* cells.

DOI: 10.1002/adma.200306253
© 2004 WILEY-VCH Verlag GmbH & Co. KGaA, Weinheim

D10488

ADVMEW
ISSN 0935-9648
Vol. 16, No. 12
June 17, 2004

ADVANCED MATERIALS

Phase Selective Chemistry in Block Copolymer Thin Films

Polymeric Networks with Antimicrobial Properties

Photovoltaic Cells of Porphyrin Dendrimers and Fullerene

Intracellular Delivery of Quantum Dots